WATER RESOURCES RESEARCH, VOL. 29, NO. 6, PAGES 1745–1752, JUNE 1993

L Moment Diagrams Should Replace Product Moment Diagrams

RICHARD M. VOGEL AND NEIL M. FENNESSEY

Department of Civil and Environmental Engineering, Tufts University, Medford, Massachusetts

It is well known that product moment ratio estimators of the coefficient of variation C_v, skewness γ, and kurtosis κ exhibit substantial bias and variance for the small ($n \leq 100$) samples normally encountered in hydrologic applications. Consequently, *L* moment ratio estimators, termed *L* coefficient of variation τ_2, *L* skewness τ_3, and *L* kurtosis τ_4 are now advocated because they are nearly unbiased for all underlying distributions. The advantages of *L* moment ratio estimators over product moment ratio estimators are not limited to small samples. Monte Carlo experiments reveal that product moment estimators of C_v and γ are also remarkably biased for extremely large samples ($n \geq 1000$) from highly skewed distributions. A case study using large samples ($n \geq 5000$) of average daily streamflow in Massachusetts reveals that conventional moment diagrams based on estimates of product moments C_v, γ, and κ reveal almost no information about the distributional properties of daily streamflow, whereas *L* moment diagrams based on estimators of τ_2, τ_3, and τ_4 enabled us to discriminate among alternate distributional hypotheses.

INTRODUCTION

The oldest and most widely understood technique for fitting frequency distributions to observed data is known as the method of moments. Method of moments estimates of a distribution's parameters are obtained by equating the sample moments with theoretical moments, resulting in a system of nonlinear equations which are often easily solved. The primary advantages of method of moments estimators include the ease with which they are computed, their conceptual simplicity, and the hope that they reproduce the theoretical moments. Traditionally, the method of moments is applied by equating the theoretical product moments

$$\mu = E[X] \tag{1a}$$

$$\sigma^2 = \text{Var}\,[X] = E[(X - \mu)^2] \tag{1b}$$

$$\gamma = \frac{E[(X - \mu)^3]}{\sigma^3} \tag{1c}$$

$$\kappa = \frac{E[(X - \mu)^4]}{\sigma^4} \tag{1d}$$

to the sample product moments

$$m = \frac{1}{n}\sum_{i=1}^{n} x_i \tag{2a}$$

$$s^2 = \left[\frac{1}{n}\sum_{i=1}^{n} (x_i - m)^2\right] \tag{2b}$$

$$G = \frac{1}{s^3}\left[\frac{1}{n}\sum_{i=1}^{n} (x_i - m)^3\right] \tag{2c}$$

$$k = \frac{1}{s^4}\left[\frac{1}{n}\sum_{i=1}^{n} (x_i - m)^4\right] \tag{2d}$$

where μ, σ^2, γ, and κ denote the theoretical mean, variance, skewness, and kurtosis, respectively, and m, s^2, G, and k denote the sample mean, variance, skewness, and kurtosis, respectively. It is well known that small sample ($n \leq 100$) estimates of s^2 and G exhibit remarkable bias and variance [*Fischer*, 1929; *Hazen*, 1930; *Wallis et al.*, 1974]. *Wallis et al.* [1974] showed that the sampling properties (bias and variance) of these product moment estimators are distribution dependent; hence subsequent efforts to develop unbiased estimators of G, for example, have met with limited success. Efforts to unbias G usually lead to skew estimators with increased variance because such unbiased estimators usually take the form αG and Var $(\alpha G) = \alpha^2$ Var (G) with $\alpha > 1$, because G is always downward biased. For a recent review of methods for unbiasing sample skewness see *Vogel and McMartin* [1991].

The remarkable small-sample bias associated with the estimator G, documented by *Wallis et al.* [1974], is only the tip of the iceberg. Monte Carlo experiments reported here reveal that both G and the coefficient of variation $C_v = s/m$ exhibit even more remarkable bias for highly skewed populations ($\gamma > 2$) and both small and large sample sizes ($n < 5000$). These experiments are performed in an effort to understand the distributional properties of daily streamflow sequences which often contain thousands of daily flows and exhibit extraordinary skewness. We found product moments to be of little value for discriminating among potential candidate distributions of daily streamflows. Another limitation of product moment estimators is that they are bounded. For example, *Kirby* [1974] shows that these bounds depend only upon sample size so that C_v is bounded by the interval $(0, (n-1)^{1/2})$ and $|G| \leq (n-2)/(n-1)^{1/2}$.

Yet still, product moment estimators are in widespread use, in part due to their availability on most calculators and in statistical software packages and textbooks, and in part due to their familiarity and commonly understood interpretation. The situation today is quite different from the situation in 1974 when *Wallis et al.* [1974] questioned the value of product moment estimators. Today a simple and attractive

Paper number 93WR00341.
0043-1397/93/93WR-00341$05.00

alternative exists: the method of L moments introduced by *Hosking* [1990]. The method of L moments is an exact analogue to the method of moments. However, L moment estimators are nearly unbiased for all sample sizes and all distributions; hence they should always be preferred in situations when unbiased moments are required, such as in the construction of moment-ratio diagrams. *Hosking* [1992] also shows that L moments are preferred to product moments in the context of evaluating the power of alternative hypothesis tests for the normal distribution. Since the theory of L moments is relatively new [*Hosking*, 1990] we outline it briefly in the following section. The remainder of the paper is devoted to comparisons between L moment and product moment ratio diagrams and to Monte Carlo experiments which reveal the remarkable bias associated with product moment ratio estimators.

The Theory of L Moments

L moments and probability weighted moments (PWMs) are analogous to ordinary moments in that their purpose is to summarize theoretical probability distributions and observed samples. Similar to ordinary product moments, L moments can be also be used for parameter estimation, interval estimation, and hypothesis testing. Although the theory and application of L moments parallel those for conventional moments, L moments have several important advantages. Since sample estimators of L moments are always linear combinations of the ranked observations, they are subject to less bias than ordinary product moments. This is because ordinary product moment estimators such as s^2 and G require squaring and cubing the observations, respectively, which causes them to give greater weight to the observations far from the mean, resulting in substantial bias and variance. *Hosking* [1990] and *Stedinger et al.* [1993] provide a summary of the theory and application of L moments. *Greenwood et al.* [1979] summarize the theory of PWMs.

Perhaps the simplest approach to describing L moments is by first defining probability weighted moments because L moments are linear functions of PWMs [*Greenwood et al.*, 1979; *Hosking*, 1990]. PWMs may be defined by

$$\beta_r = E\{X[F_X(x)]^r\} \tag{3}$$

where $F_X(x)$ is the cumulative distribution function of X. When $r = 0$, β_0 is the mean streamflow μ defined earlier in (1*a*). Hence a sample estimate of the first PWM, which we term b_0, is given by m in (2*a*). All higher-order PWMs are simply linear combinations of the order statistics $X_{(n)} \leq \cdots \leq X_{(1)}$.

Landwehr et al. [1979] recommends the use of biased estimates of PWMs and L moments, since such estimators often produce quantile estimates with lower root-mean-square error than unbiased alternatives. Nevertheless, unbiased estimators are often preferred in goodness of fit evaluations such as L moment diagrams. Unbiased estimators are preferred because they have less bias for estimating τ_3 and τ_4, and they are invariant if the data are multiplied by a constant, which is not the case for the biased estimators. Unbiased sample estimates of the PWMs, for any distribution can be computed from

$$b_0 = m = \frac{1}{n}\sum_{j=1}^{n} x_j \tag{4a}$$

$$b_1 = \sum_{j=1}^{n-1}\left[\frac{(n-j)}{n(n-1)}\right]x_{(j)} \tag{4b}$$

$$b_2 = \sum_{j=1}^{n-2}\left[\frac{(n-j)(n-j-1)}{n(n-1)(n-2)}\right]x_{(j)} \tag{4c}$$

$$b_3 = \sum_{j=1}^{n-3}\left[\frac{(n-j)(n-j-1)(n-j-2)}{n(n-1)(n-2)(n-3)}\right]x_{(j)} \tag{4d}$$

where $x_{(j)}$ represents the ordered streamflows with $x_{(1)}$ being the largest observation and $x_{(n)}$ the smallest. The PWM estimators in (4) can be more generally described using

$$b_r = \frac{1}{n}\sum_{j=1}^{n-r}\left[\frac{\binom{n-j}{r}}{\binom{n-1}{r}}\right]x_{(j)} \tag{5}$$

For any distribution, the first four L moments are easily computed from the PWMs using

$$\lambda_1 = \beta_0 \tag{6a}$$

$$\lambda_2 = 2\beta_1 - \beta_0 \tag{6b}$$

$$\lambda_3 = 6\beta_2 - 6\beta_1 + \beta_0 \tag{6c}$$

$$\lambda_4 = 20\beta_3 - 30\beta_2 + 12\beta_1 - \beta_0 \tag{6d}$$

The first four unbiased L moment sample estimators are obtained by substituting the PWM sample estimators b_r from (4) into the L moment equations in (6). Equations (6*a*)–(6*d*) are special cases of the general recursion

$$\lambda_{r+1} = \sum_{k=0}^{r}\beta_r(-1)^{r-k}\binom{r}{k}\binom{r+k}{k} \tag{7}$$

A computer program is available for implementing the method of L moments [*Hosking*, 1991*b*]. In the following sections we briefly define L moment ratios, discuss their relationship to conventional moments, and introduce L moment diagrams.

L Moment Ratios and the Interpretation of L Moments

Analogous to the product moment ratios, coefficient of variation $C_v = \sigma/\mu$, skewness γ, and kurtosis κ, *Hosking* [1990] defines the L moment ratios

$$\tau_2 = \frac{\lambda_2}{\lambda_1} \equiv L \text{ coefficient of variation} \tag{8a}$$

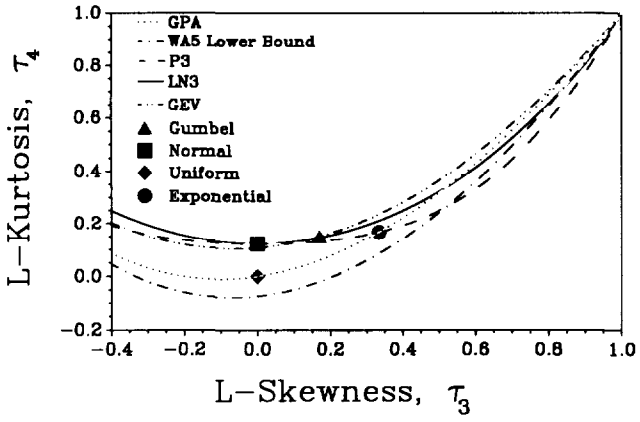

Fig. 1. An L moment diagram which describes the theoretical relationships between L kurtosis and L skewness for the exponential, uniform, normal, Gumbel, Pearson type 3 (P3), three-parameter lognormal (LN3), generalized Pareto (GPA), Generalized Extreme Value (GEV), and the lower bound of the five-parameter Wakeby (WA5) distributions.

$$\tau_3 = \frac{\lambda_3}{\lambda_2} \equiv L \text{ skewness} \tag{8b}$$

$$\tau_4 = \frac{\lambda_4}{\lambda_2} \equiv L \text{ kurtosis} \tag{8c}$$

where λ_r, $r = 1, \cdots, 4$ are the first four L moments and τ_2, τ_3, and τ_4 are the L coefficient of variation (L-C_v), L skewness, and L kurtosis, respectively. The first L moment λ_1 is equal to the mean streamflow μ, hence it is a measure of location. *Hosking* [1990] shows that λ_2, τ_3, and τ_4 can be thought of as measures of a distributions scale, skewness, and kurtosis, respectively, analogous to the ordinary moments σ, γ, and κ, respectively.

Moment Ratio Diagrams

Conventional product moment ratio diagrams compare the sample estimates of the product moment ratios $C_v = s/m$, G, and k with their theoretical counterparts σ/μ, γ, and κ for a range of assumed distributions. *McCuen* [1985] provides an introduction to product moment ratio diagrams. Similarly, L moment ratio diagrams introduced by *Hosking* [1990] compare sample estimates of the dimensionless ratios τ_2, τ_3, and τ_4 with their population counterparts for a range of assumed distributions. A significant advantage of moment ratio diagrams is that one can compare the fit of several distributions using a single graphical instrument. For example, Figure 1 displays the theoretical relationships between L kurtosis τ_4 and L skewness τ_3 for the normal, Gumbel, exponential, uniform, three-parameter lognormal (LN3), Pearson type 3 (P3), generalized Pareto (GPA), generalized extreme value (GEV), and the lower bound of the five-parameter Wakeby (WA5) distributions. Here one observes the tremendous flexibility of the three-parameter distributions (LN3, P3, GPA, and GEV) in comparison to the two-parameter alternatives. The five-parameter Wakeby distribution is the most flexible distribution considered since it defines a two-dimensional region in Figure 1 rather than a curve or a point as is the case for the three- and two-parameter distributions, respectively (see *Kotz and Johnson* [1988] for a summary of the Wakeby distribution). The theoretical relationships between τ_4 and τ_3 depicted in Figure 1 were obtained from the polynomial approximations developed by *Hosking* [1991*a*] and summarized in the work by *Stedinger et al.* [1993]. *Stedinger et al.* [1993] also describe the theoretical properties of these distributions.

Hosking [1990] introduced L moment diagrams for the purpose of selecting a suitable pdf for modeling hydrologic variables at many sites. Examples of L moment diagrams can be found in the works by *Wallis* [1988, 1989], *Hosking* [1990], *Hosking and Wallis* [1987*a*, 1991], and *Vogel et al.* [1993*a*, *b*]. For example, *Hosking and Wallis* [1987*a*] found L moment diagrams useful for selecting the GEV distribution over the gamma distribution for modeling annual maximum hourly rainfall data. Similarly, *Wallis* [1988, Figure 3] found an L moment diagram useful for rejecting *Jain and Singhs* [1987] conclusion that annual maximum floodflows at 44 sites were well approximated by a Gumbel distribution and for suggesting a GEV distribution instead. *Vogel et al.* [1993*a*] used L moment diagrams to show that floodflows at 383 sites in southwestern United States were equally well approximated by the LP3, LN3, and GEV distributions. *Vogel et al.* [1993*b*] used L moment diagrams to show that floodflows were well approximated by a GEV distribution in the regions of Australia which receive most rainfall during winter months and by a GPA distribution in the regions of Australia which receive most rainfall during summer months.

L moment diagrams are clearly useful for evaluating which distribution(s), among a suite of possible models, provides a satisfactory approximation to the distribution of a particular hydrologic variable in a region.

A Comparison of L Moment and Product Moment Ratio Diagrams

In this section we evaluate the use of product-moment ratio diagrams for selecting a suitable probability density function (pdf) for modeling the frequency and magnitude of average daily streamflow in Massachusetts. Selection of a suitable pdf for average daily streamflow is important in studies which seek to develop regional hydrologic models for describing daily streamflow duration curves (see *Fennessey and Vogel* [1990] for a recent review of the literature on regional flow duration curves). Daily streamflow duration curves are used routinely for solving a wide range of water resource engineering problems including, but not limited to, hydropower feasibility analyses, wasteload allocation, river and reservoir sedimentation, water quality management, and the determination of instream flow requirements. Streamflow duration curves for ungaged basins are often obtained using regional hydrologic procedures which require an assumption regarding the distributional properties of daily streamflow in a region. The following experiments document that in spite of the complexity of the physical processes which generate daily streamflow, it may be reasonable to approximate the distributional behavior of daily streamflow using a simple three-parameter probability distribution, in Massachusetts.

L moment ratio and product-moment ratio diagrams are constructed using average daily streamflows for 23 of the U.S. Geological Survey's streamflow-gaging stations in Massachusetts with the following attributes.

TABLE 1. Characteristics of Streamflow Records of 23 Massachusetts Sites

USGS Gage Number	Site	Years of Record	Area, mi^2	Mean m, cfs	L Moment Ratios			Product Moment Ratios		
					τ_2	τ_3	τ_4	C_v	G	k
1180500	1	51	52.70	107.8	0.616	0.543	0.348	1.77	8.69	165.8
1096000	2	40	63.69	111.6	0.550	0.461	0.273	1.37	5.35	59.1
1106000	3	37	8.01	14.3	0.581	0.417	0.248	1.35	3.83	27.0
1170100	4	22	41.39	91.2	0.579	0.522	0.329	1.52	5.21	49.4
1174000	5	34	3.39	6.1	0.583	0.446	0.266	1.42	4.78	46.9
1175670	6	29	8.68	14.7	0.554	0.418	0.243	1.30	4.20	33.3
1198000	7	19	51.00	78.6	0.585	0.472	0.270	1.41	4.08	29.8
1171800	8	11	5.46	7.7	0.524	0.421	0.228	1.15	2.79	13.9
1174900	9	28	2.85	4.9	0.593	0.503	0.344	1.64	6.11	66.7
1101000	10	44	21.30	36.9	0.568	0.389	0.192	1.22	3.12	23.3
1187400	11	31	7.35	14.0	0.627	0.536	0.361	2.35	27.83	1429.2
1169000	12	50	89.00	185.5	0.605	0.548	0.359	1.71	6.85	91.1
1111300	13	25	16.02	30.8	0.580	0.454	0.277	1.47	5.64	63.0
1169900	14	23	24.09	52.5	0.561	0.511	0.334	1.57	6.67	76.4
1181000	15	54	94.00	190.6	0.611	0.541	0.356	1.82	8.88	154.2
1332000	16	58	40.90	96.6	0.590	0.540	0.356	1.63	6.52	87.3
1097300	17	26	12.31	20.7	0.579	0.436	0.231	1.34	4.42	43.1
1333000	18	40	42.60	82.5	0.542	0.463	0.283	1.33	4.79	45.1
1165500	19	65	12.10	20.0	0.590	0.485	0.285	1.49	5.82	82.1
1171500	20	51	54.00	96.5	0.557	0.491	0.304	1.47	6.41	84.0
1176000	21	77	150.00	244.9	0.487	0.367	0.187	1.07	5.47	97.6
1162500	22	53	19.30	32.6	0.597	0.489	0.291	1.54	8.73	252.0
1180000	23	28	1.73	2.6	0.620	0.512	0.311	1.74	9.99	231.4

Here, mi^2 denotes square miles; 1 mi^2 = 2.590 × 10^6 m^2; cfs denotes cubic feet per second; 1 cfs = 28.32 L/s.

1. All of the rivers are perennial.
2. No significant withdrawals, diversions, or artificial recharge areas are contained in the basins; hence we consider these streamflows to be essentially unregulated.
3. The streamflow records range in length from 11 to 77 years, typical of a wide range of regional samples encountered in practice.

The U.S. Geological Survey Station numbers, record lengths, drainage areas, L moment ratio, and product-moment ratio estimates are summarized in Table 1. Further information regarding these 23 sites, including selected streamflow statistics, other drainage basin characteristics and a location map is included in studies by *Vogel and Kroll* [1990, 1992] and *Fennessey and Vogel* [1990].

L Moment Ratio Diagrams for Daily Streamflows in Massachusetts

Figure 2 (top) is an L moment diagram which uses solid circles to illustrate the relation between sample estimates of L kurtosis and sample estimates of L skewness, computed from the complete records of daily streamflow at the 23 basins in Massachusetts. For comparison, the curves reveal the theoretical relationships between L kurtosis and L skewness for the LN3, GEV, P3, GPA, and the lower bound for the WA5 distribution. Sample estimates of L skewness and L kurtosis are obtained using the unbiased L moment estimators given in (4), (6), and (8). Even though estimates of the L moments λ_r, r = 1, 2, 3, and 4 are unbiased, this does not imply that the sample ratio estimators L-C_v, L skewness, and L kurtosis are unbiased.

Of all the three-parameter models tested in Figure 2 (top), the generalized Pareto (GPA) model provides the best approximation to the observed daily streamflows. When one compares the overall behavior of L moment diagrams for these distributions in Figure 1 to the results in Figure 2 (top), one observes the remarkable ability of L moment diagrams for distinguishing among relatively similar distributional hypotheses. We conclude from Figure 2 (top) that the GPA distribution provides a better overall approximation to the distribution of daily streamflows in Massachusetts than the LN3, GEV, P3, Gumbel, normal, uniform, or exponential models. Since the GPA distribution is a special case of the WA5 distribution, one would expect the WA5 distribution to provide the best fit among all models compared in Figure 2, at the expense of having to estimate two additional parameters.

Figure 2 (bottom) is an L moment diagram which illustrates sample estimates of L-C_v τ_2, versus sample estimates of L skewness τ_3, for the same sites as in Figure 2 (top). For comparison, we plot the theoretical relationship (using a solid line) between τ_2 and τ_3 corresponding to the two-parameter GPA distribution. *Hosking and Wallis* [1987*b*], *Stedinger et al.* [1993], and *Vogel et al.* [1993*b*] describe the theoretical properties of the two- and three-parameter GPA distribution. The two-parameter GPA distribution is equivalent to the three-parameter version with the lower bound ξ, set to zero. The two-parameter GPA distribution provides a good approximation to the relationship between L-C_v and L skewness for this region.

Comparison of Product Moment Ratio and L Moment Ratio Diagrams for Daily Streamflows in Massachusetts

The immediate question which arises in the mind of anyone who has not experienced the value of L moment diagrams is, Would the use of conventional product moment

ratio diagrams lead to the same conclusions as the use of L moment ratio diagrams?. In Figures 3 and 4 we compare the use of L moment ratio diagrams with conventional product moment ratio diagrams, using the same Massachusetts sites as in Table 1 and Figure 2. In all cases, the open circles denote the use of the complete period of record, and the solid circles denote the use of the complete period of record without the largest observation. One would expect the sample estimates of both L moment ratios and conventional product moment ratios to be relatively insensitive to the largest observation, since we are dealing with samples with thousands, and at some sites, tens of thousands of daily streamflow observations. As expected, the L moment ratio diagrams depicted in Figures 3 (top) and 4 (top) are relatively unaffected by dropping the largest observation. However, the conventional product moment ratio diagrams illustrated in Figures 3 (bottom) and 4 (bottom) are significantly impacted by dropping the largest observation. Dropping the largest observation should tend to reduce the estimated kurtosis, skewness, C_v, L kurtosis, L skewness, and L-C_v, since it is the large observations which tend to cause skewness (in a positively skewed population). This is exactly the effect we observe in the L moment diagrams in Figures 3 (top) and 4 (top); all the points are shifted down and to the left when the largest observation is removed. Yet the conventional product moments behave much more unpredictably. In some instances dropping the largest observation leads to remarkable reductions in kurtosis and skewness (note kurtosis is plotted using a logarithmic axis), yet in other instances the sample estimates are not noticeably affected. Hence it is not surprising that the sample product moment ratios are in poor agreement with the theoretical relationships for the GPA distribution illustrated in Figures 3 (bottom) and 4 (bottom). Apparently, estimated sample values of C_v, γ, and κ are highly biased even when one is dealing with thousands of highly skewed observations. This should not be too surprising given the results of simulation experiments performed by *Wallis et al.* [1974] which indicated that the variance of estimates of the skew coefficient often increased with sample size for highly skewed populations. This is exactly the effect we are observing.

Overall, the conventional product moment ratio diagrams in Figures 3 (bottom) and 4 (bottom) do not reveal any agreement between the theoretical distributions and the sample product moment ratios. Monte Carlo experiments, performed in the next section reveal that sample estimates of the product moment ratios C_v and G are remarkably downward biased for highly skewed samples, even for samples sizes in the range n = 1000 to 5000. Hence the results of Figures 3 and 4 are to be expected given knowledge of the sampling properties of product moment ratio estimators for highly skewed samples.

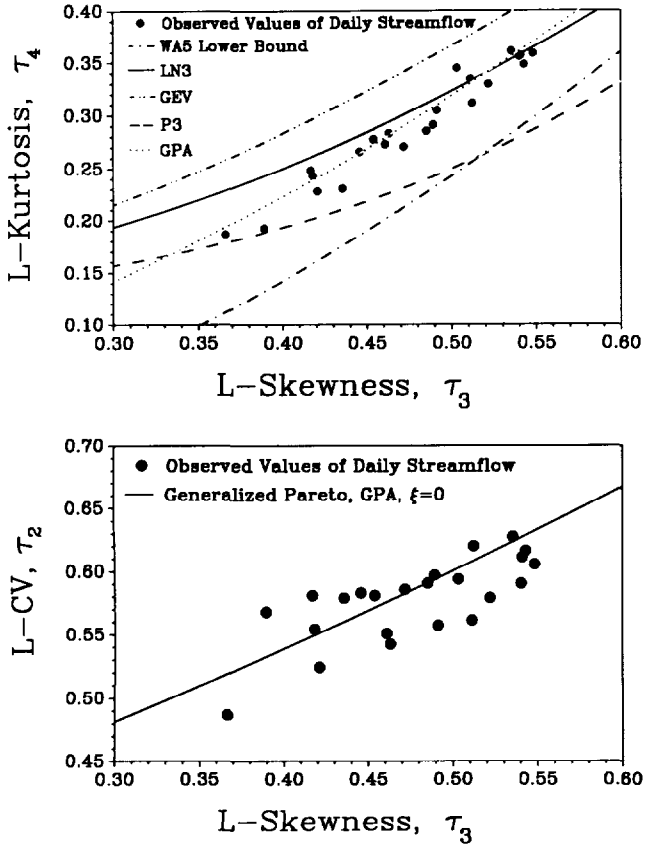

Fig. 2. L moment diagrams describing the sample and theoretical relationships between (top) L kurtosis τ_4 and L skewness τ_3 and (bottom) L coefficient of variation τ_2 and L skewness τ_3 for average daily streamflows at the 23 sites in Massachusetts, summarized in Table 1.

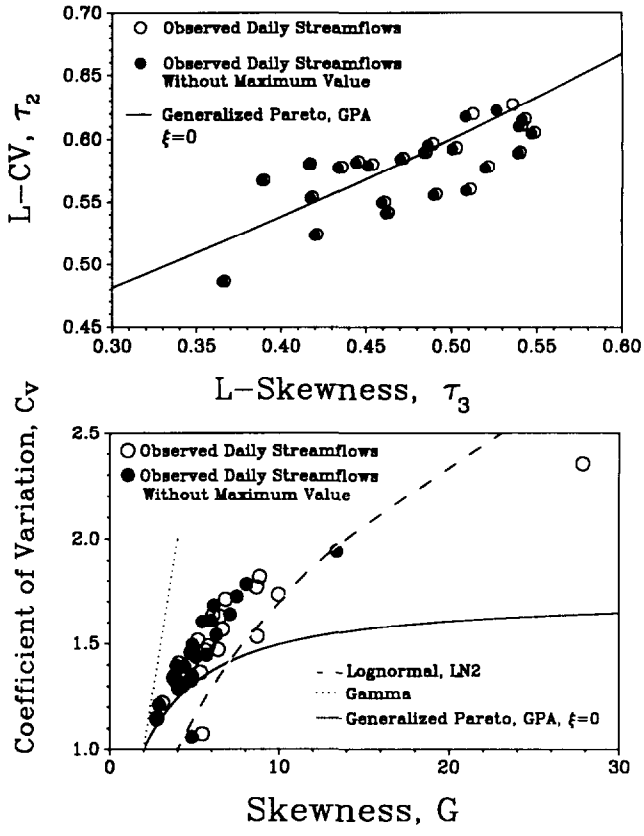

Fig. 3. (Top) L moment ratio diagram comparing the sample and GPA theoretical relationship between L-C_v, τ_2 and L skewness τ_3 and (bottom) product moment ratio diagram comparing the sample and GPA theoretical relationship between coefficient of variation C_v and skewness G, using average daily streamflows at the 23 sites in Massachusetts, summarized in Table 1.

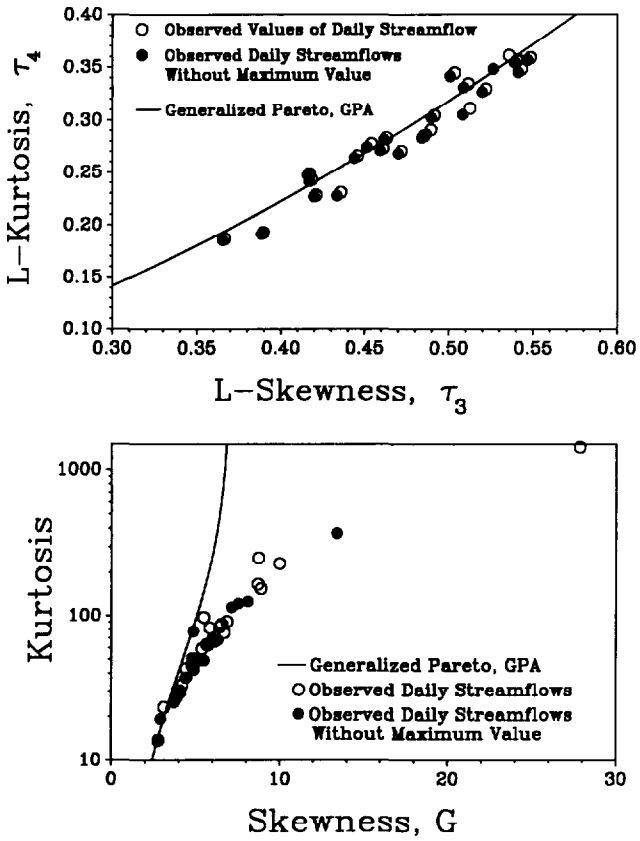

Fig. 4. (Top) L moment diagram comparing the sample and GPA theoretical relationship between L kurtosis τ_4 and L skewness τ_3 and (bottom) product moment diagram comparing the sample and GPA theoretical relationship between kurtosis k and skewness G, using average daily streamflows at the 23 sites in Massachusetts, summarized in Table 1.

A Few Caveats

One might object to the previous analyses because it could be argued that a sensible hydrologist would never attempt to estimate product moments for highly skewed data. Instead, a suitable logarithmic or Box-Cox transformation might be applied to the highly skewed daily streamflows, removing some of the excessive skew in the data, allowing the product moments a chance to behave more reasonably. However, if our goal is to evaluate the goodness of fit of alternative distributions, transforming the data only assists us in determining the distribution of the transformed data, instead of the original data.

We constructed L moment and product-moment diagrams similar to Figures 2–4 by first taking logarithms of all the daily streamflows. Since the conclusions derived from those diagrams are not central to our paper, we did not include them. We found that both L moment diagrams and product moment diagrams based on the logarithms of the daily streamflows revealed that the logarithms are neither well approximated by a normal distribution or a P3 distribution. Hence taking logarithms only allowed us to conclude that daily streamflows in Massachusetts are poorly approximated by a lognormal and a log Pearson type 3 (LP3) distribution. Taking logarithms would have never enabled us to determine that daily streamflows are well approximated by a GPA distribution in Massachusetts, as we found in Figures 2–4.

THE SAMPLING PROPERTIES OF ESTIMATES OF PRODUCT MOMENT RATIOS

In the previous section we showed that product moment ratio diagrams are remarkably sensitive to the largest streamflow observations and such diagrams led to different conclusions than L moment ratio diagrams. Thus far, our attention focused on observed daily flow data for which the underlying pdf is unknown, hence we were unable to provide a definitive explanation for this discrepancy. In this section we perform a Monte Carlo experiment which proves that sample product moment estimators of C_v and γ exhibit significant downward bias, even for extremely large sample sizes. This bias tends to increase with both C_v and γ, which explains the phenomenon we observed in Figures 3 (bottom) and 4 (bottom).

MONTE CARLO EXPERIMENTS

Experimental Design

All of the experiments follow the same general procedure. First, 10,000 sets of streamflow traces are generated of length n from a two-parameter lognormal (LN2) and a two-parameter generalized Pareto (GPA) model. Streamflow traces of length n = 10, 20, 50, 100, 200, 500, 1000, and 5000 are generated from LN2 and GPA populations with C_v = 1, 2, 5, and 10. This parameter space is intended to capture the range of variability in both n and C_v which is typical of daily streamflow sequences. Note that even if one has a sample of 10,000 daily streamflows, the effective record length of those observations may be less than 1000 when one accounts for the loss in information due to the serial correlation of the flow records. For each streamflow trace, the sample estimators $C_v = s/m$ and G are obtained using (2). Next we compute

$$\text{Bias } (C_v) = \sigma/\mu - E[C_v],$$

$$\text{Bias } (G) = \gamma - E[G],$$

$$\text{rmse } (C_v) = \{[\text{Bias } (C_v)]^2 + \text{Var } (C_v)\}^{1/2} \text{ and}$$

$$\text{rmse } (G) = \{[\text{Bias } (G)]^2 + \text{Var } (G)\}^{1/2}.$$

Note that we do not compute either the Bias(G) or rmse(G) for the GPA distribution, since the skewness of the GPA distribution is undefined for most values of C_v considered here (i.e., γ is undefined for $C_v > 1.73$). Note that even though the skewness of the GPA distribution is undefined for most values of C_v considered here, L moments are still meaningful; another important advantage of L moments over product moments. The results are reported in Figures 5 and 6.

Results

Figure 5 summarizes Bias(C_v) and rmse(C_v) as a fraction of the true value C_v versus sample size n and population C_v, for LN2 and GPA observations. Similarly, Figure 6 summarizes Bias(G) and rmse(G) as a fraction of the true value γ, versus sample size n and population γ, for LN2 observations. What is most revealing about these results is that the bias of both C_v and G is extraordinary for samples with values of C_v in excess of 5, even for sample sizes in excess

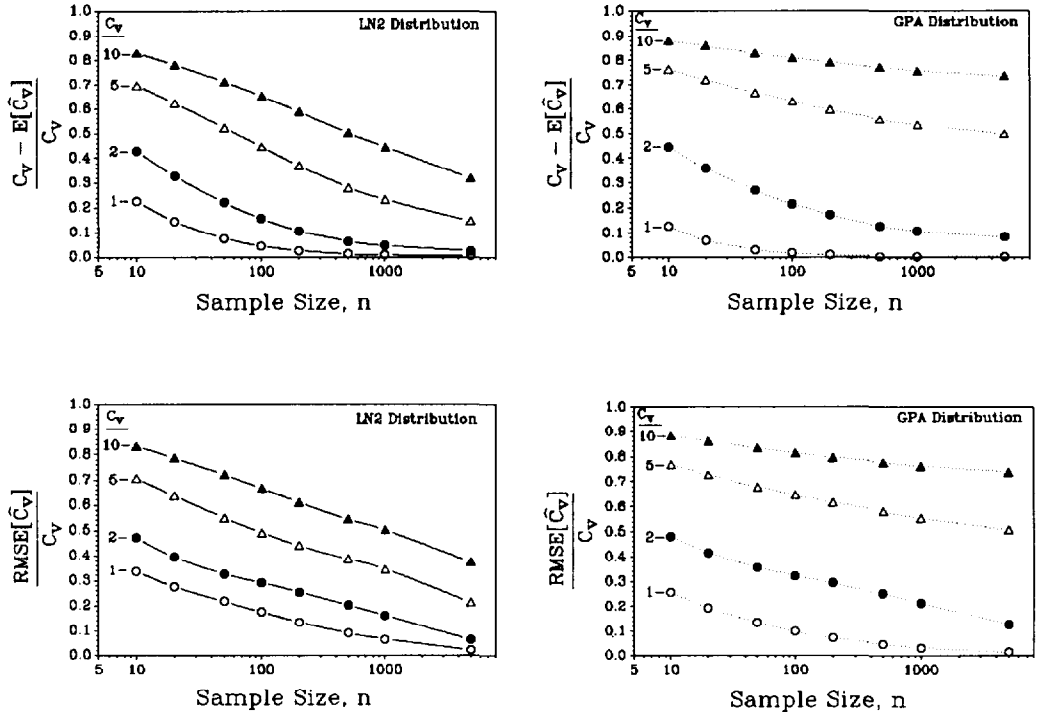

Fig. 5. The bias and rmse of product moment estimates of C_v (as a fraction of the true value of C_v) are illustrated as a function of sample size n and the population value of C_v for two-parameter lognormal (LN2) samples and two-parameter generalized Pareto (GPA) samples. Each point in the figure is based on 10,000 replicate experiments.

of 1000. Apparently, as the population values of both C_v and γ increase, even large sample estimates of product moment ratios contain almost no information about either the coefficient of variation or the skewness of the samples. Furthermore, the root-mean-square error (rmse) of both estimators C_v and G are generally dominated by bias, and since this bias disappears very slowly with sample size, the rmse of both C_v and G also disappears very slowly for highly skewed samples. It is also clear from Figure 5 that the sampling properties of estimates of C_v are quite different for the LN2 and GPA populations, hence efforts to derive unbiased estimators of C_v would require distributional assumptions. Since our earlier objective was to employ moment ratio diagrams for selecting a suitable distribution for daily flows, use of unbiased product moment estimators would be troublesome because a distributional assumption is required to develop unbiased product moment estimators (a chicken and egg problem).

The bias associated with both estimators C_v and G results from the fact that these product moment estimators require squaring and cubing of the differences between each observation and the sample mean. As was shown in Figures 3 and 4, the sum of the square, cube, and fourth power of the difference between the observations and their sample mean is dominated by the few extraordinarily large observations typical of most highly skewed daily flow records. Hence one expects the bias and rmse of G to be much greater than the bias and rmse of C_v, as is observed in Figures 5 and 6. Similarly, one expects the bias and rmse associated with product moment estimates of kurtosis to be still greater; however, we elected not to compute it since our results for C_v and γ provide sufficient evidence to discontinue the use of product moment estimators for highly skewed samples.

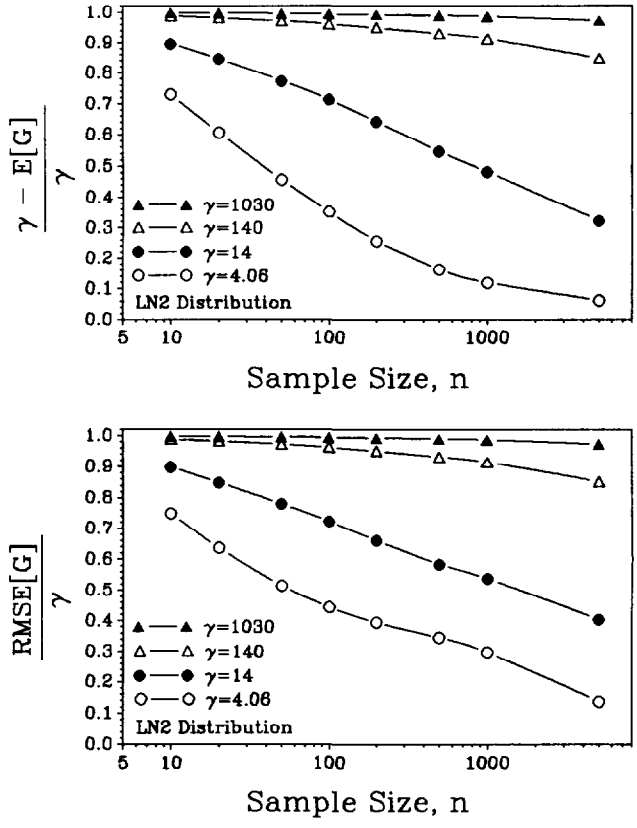

Fig. 6. The bias and rmse of product moment estimates of skewness G (as a fraction of the true value, γ) are illustrated as a function of sample size n and the population value γ for two-parameter lognormal (LN2) samples. Each point in the figure is based on 10,000 replicate experiments.

CONCLUSIONS

A comparison of conventional product moment ratio and L moment ratio diagrams in Figures 3 and 4 illustrates how remarkably sensitive sample estimates of the coefficient of variation C_v, skewness G, and kurtosis k are to the large observations often associated with long records of daily streamflow. A Monte Carlo experiment documented (see Figures 5 and 6) the significant downward bias associated with large-sample estimates of C_v and G for lognormal and generalized Pareto samples. Combining the results of our large-sample Monte Carlo experiments in Figures 5 and 6, with the extensive small-sample computer experiments performed by *Wallis et al.* [1974], we conclude that product moment estimates of C_v and γ should be replaced by L moment estimators for most goodness of fit applications in hydrology including both small-sample, low-C_v applications [see *Wallis et al.*, 1974] and both small- and large-sample, high-C_v applications.

There are two general situations in which relatively unbiased product moment estimators are available. When one transforms the observations by taking logarithms, product moment estimators will behave similarly to L moment estimators. Unfortunately, transforming the data will not usually assist us in determining the distributional properties of the original data except in special cases such as the LP3 and LN3 distributions. Furthermore, streamflow cannot always be transformed by taking logarithms, since many flow sequences contain zeros. Another situation in which relatively unbiased product moment estimators are available is in large-sample, low-C_v applications; however, such situations are not usually encountered in hydrology.

We conclude that for the purpose of constructing moment diagrams in hydrology, L moment diagrams are always preferred over product moment diagrams because the L moment ratios L-C_v, L skewness, and L kurtosis are nearly unbiased for all combinations of sample size and C_v and for all populations [*Hosking*, 1990].

Acknowledgments. The authors gratefully acknowledge the financial support of the U.S. Geological Survey who sponsored this research under the terms of contract 14-08-0001-G2071 titled The Application of Streamflow Duration Curves in Water Resources Engineering. In addition, the authors acknowledge the financial support of the Tufts University Center for Environmental Management. The authors are also grateful to J. R. M. Hosking for providing useful comments on an early version of this manuscript. The views and conclusions contained in this document are those of the authors and should not be interpreted as necessarily representing the official policies, either expressed or implied of the U.S. Government.

REFERENCES

Fennessey, N. M., and R. M. Vogel, Regional flow-duration curves for ungauged sites in Massachusetts, *J. Water Resour. Plann. Manage., Div. Am. Soc. Civ. Eng.*, *116*(4), 530–549, 1990.

Fischer, R. A., Moments and product moments of sampling distributions, *R. London Math. Soc.*, *2*(30), 199, 1929.

Greenwood, J. A., J. M. Landwehr, N. C. Matalas, and J. R. Wallis, Probability weighted moments: Definition and relation to parameters of several distributions expressible in inverse form, *Water Resour. Res.*, *15*(5), 1049–1054, 1979.

Hazen, A., *Flood Flows*, John Wiley, New York, 1930.

Hosking, J. R. M., L-moments: Analysis and estimation of distributions using linear combinations of order statistics, *J. R. Stat. Soc., Ser. B*, *52*(2), 105–124, 1990.

Hosking, J. R. M., Approximations for use in constructing L-moment ratio diagrams, *Res. Rep. RC-16635*, 3 pp., IBM Res. Div., T. J. Watson Res. Cent., Yorktown Heights, N. Y., 1991*a*.

Hosking, J. R. M., Fortran routines for use with the method of L-moments, Version 2, *Res. Rep. RC-17097 (#75864)*, 117 pp., IBM Res. Div., T. J. Watson Res. Cent., Yorktown Heights, N. Y., 1991*b*.

Hosking, J. R. M., Moments or L moments? An example comparing two measures of distributional shape, *Am. Stat.*, *46*(3), 186–189, 1992.

Hosking, J. R. M., and J. R. Wallis, An "index-flood" procedure for regional rainfall frequency analysis, *Eos Trans. AGU*, *68*, 312, 1987*a*.

Hosking, J. R. M., and J. R. Wallis, Parameter and quantile estimation for the generalized Pareto distribution, *Technometrics*, *29*(3), 339–349, 1987*b*.

Hosking, J. R. M., and J. R. Wallis, Some statistics useful in regional frequency analysis, *Res. Rep. RC 17096*, 23 pp., IBM Res. Div., T. J. Watson Res. Cent., Yorktown Heights, N. Y., 1991.

Jain, D., and V. P. Singh, Estimating parameters of EVI distribution for flood frequency analysis, *Water Resour. Bull.*, *23*(1), 59–71, 1987.

Kirby, W., Algebraic boundedness of sample statistics, *Water Resour. Res.*, *10*(2), 220–222, 1974.

Kotz, S., and N. L. Johnson, *Encyclopedia of Statistical Sciences*, vol. 9, pp. 513–514, John Wiley, New York, 1988.

Landwehr, J. M., N. C. Matalas, and J. R. Wallis, Probability weighted moments compared with some traditional techniques in estimating Gumbel parameters and quantiles, *Water Resour. Res.*, *15*(5), 1055–1064, 1979.

McCuen, R. H., *Statistical Methods for Engineers*, pp. 61–63, Prentice-Hall, Englewood Cliffs, N. J., 1985.

Stedinger, J. R., R. M. Vogel, and E. Foufoula-Georgiou, Frequency analysis of extreme events, in *Handbook of Applied Hydrology*, chapt. 18, editor-in-chief D. A. Maidment, McGraw-Hill, New York, 1993.

Vogel, R. M., and C. N. Kroll, Generalized low-flow frequency relationships for ungaged sites in Massachusetts, *Water Resour. Bull.*, *26*(2), 241–253, 1990.

Vogel, R. M., and C. N. Kroll, Regional geohydrologic-geomorphic relationships for the estimation of low-flow statistics, *Water Resour. Res.*, *28*(9), 2451–2458, 1992.

Vogel, R. M., and D. E. McMartin, Probability plot goodness-of-fit and skewness estimation procedures for the Pearson type 3 distribution, *Water Resour. Res.*, *27*(12), 3149–3158, 1991.

Vogel, R. M., W. O. Thomas, and T. A. McMahon, Floodflow frequency model selection in Southwestern U.S.A., *J. Water Resour. Plann. Manage., Div. Am. Soc. Civ. Eng.*, *119*(3), 353–366, 1993*a*.

Vogel, R. M., T. A. McMahon, and F. H. S. Chiew, Floodflow frequency model selection in Australia, *J. Hydrol.*, in press, 1993*b*.

Wallis, J. R., N. C. Matalas, and J. R. Slack, Just a moment, *Water Resour. Res.*, *10*(2), 211–219, 1974.

Wallis, J. R., Catastrophes, computing and containment: Living in our restless habitat, *Spec. Sci. Tech.*, *11*(4), 294–315, 1988.

Wallis, J. R., Regional frequency studies using L-moments, *Res. Rep. 14597*, 17 pp., IBM Res. Div., T. J. Watson Res. Cent., Yorktown Heights, N. Y., 1989.

N. M. Fennessey and R. M. Vogel, Department of Civil and Environmental Engineering, Tufts University, Medford, MA 02155.

(Received August 19, 1992;
revised February 4, 1993;
accepted February 5, 1993.)